bioRχiv

Starling murmurations under predation

Marina Papadopoulou[a,b,*] Hanno Hildenbrandt[a], Rolf F. Storms[a], and Charlotte K. Hemelrijk[a]
[a] Groningen Institute for Evolutionary Life Sciences, University of Groningen, Groningen, The Netherlands
[b] Department of Biosciences, Faculty of Science and Engineering, Tuscia University, Viterbo, Italy
*m.papadopoulou.rug@gmail.com

Abstract

European starlings perform a great diversity of patterns of collective behaviour when hunted by aerial predators; their large flocks are changing shape, size, and internal structure continuously and rapidly, but how these patterns emerge by self-organization is still unknown. Here, we disentangle the emergence of several interconnected patterns of collective escape in starlings. We combine video footage of starling flocks pursued by a robotic predator, the RobotFalcon, with simulations of large flocks in a new data-driven 3-dimentional agent-based model. Our empirical data show that flock members often differ in their evasive manoeuvres and that several patterns of collective escape arise simultaneously at different parts in the flock. In our computational model, we identify what rules of motion, coordination and escape at the individual level lead to the emergence of group density, internal dynamics, and patterns of collective escape similar to real starling flocks. Overall, our results suggest that the emergence and dynamics of simultaneous patterns of collective escape depend on: the speed with which the escape information propagates from one or few initiators, the positions of the escaping flock members in relation to the predator, and the previous state of the flock (hysteresis).

Keywords: collective escape; self-organization; European starling; flocking; predation; agent-based modeling; hysteresis.

Introduction

Some of the most complex patterns of collective behavior in animals are displayed when groups are under predation. Rapid changes in shape and internal structure of the group confuse the predator[1,2] and reduce the individuals' risk of getting caught[3,4]. The murmurations of European starlings (*Sturnus vulgaris*)[5] are perhaps the most well-known phenomenon of collective behavior in nature[5,6], because of their large flocks and great diversity of patterns, in particular when attacked by aerial predators such as the peregrine falcon (*Falco peregrinus*)[7,8]. However, little is known about what rules of motion and interaction underlie their emergent patterns of collective escape[9], knowledge that is vital to understand the adaptive value of these social interactions and the behavioral mechanism of their collective intelligence.

Empirical scientists have classified many patterns of collective escape, namely the agitation wave, the vacuole, the flash expansion, the collective turn, the cordon, the split, compacting and dilution[8], according to the shape, darkness, size and internal structure of the flock, as well as its dynamics [7,10]. During an agitation wave, a dark band moves from one side of the flock (closer to the predator) to the other[8,11]. The flash expansion implies that flock members move suddenly radially outwards (usually away from the attacking predator)[8,12]. The split implies that the flock divides into two or more parts, referred to as sub-flocks[8,13]. During blackening, the flock (or part of it) appears darker, and during compacting smaller[8], with a common overlap between the two. During dilution, the distance between flock members increases and the flock appears lighter in color[8]. The vacuole refers to a hole in a polarized flock with the individuals around the hole moving in the same direction, and the cordon to the thin line (cordon) that connects two relatively large parts of the flock[7,8]. Most studies have so far investigated the relation between the frequency of some of these patterns and the frequency and timing of predator attacks[7,8,11], but more in depth investigations on the mechanism of their emergence have been hampered by the difficulty to collect data of starling flocks in the field[14].

Protocols for data collection must overcome the high altitude in which starling flocks fly when under attack, their large flock size, the long duration of their collective escape, and the unpredictability of predator attacks in nature. First, because of their large spatial distance from ground cameras during video observations[7,8,11,14], the individuals' motion cannot be observed directly[11]. Second, existing techniques to collect data of individuals' motion in a group through 3D imaging are not yet suitable to study murmurations: they use a stable frame of cameras and collect data on the few seconds of flight that the flock happens to pass through the frame[14]. Thus, they cannot capture the whole flock and the predator for the whole duration of a pursuit, given that the flock quickly moves outside the camera frame. Lastly, relying on natural predators attacking flocks at the exact location of a field study makes the collection of enough data extremely challenging. As a result, tracking data of flocks during collective escape are scarce[15].

This lack of empirical data has constrained the development of computational models of bird flocks[9,13,16–21]. Models of collective behavior based on self-organization usually include moving agents that align with and are attracted to each other

while avoiding collisions[22]. In these models, several properties of collective motion have been examined, for instance flock diffusion[23,24], milling[17,25], and group shape[26,27]. However, only a few types of collective escape in bird flocks have been studied in detail[9,13,21,28], using two computational models, one of starlings (named *StarDisplay*[20]) and one of homing pigeons (*Columba livia*, named *HoPE*[13]). *StarDisplay* was used to study agitation waves, and showed that they may emerge from a fixed zig-zag motion performed by a few individuals close to the predator and copied by their neighbors[9]. *HoPE* showed that splits and collective turns in pigeons emerged from individual escape maneuvers: discrete, sudden turns interrupting the continuous coordinated motion of the group[13]. Across taxa, most computational models to date focus on the emergence of a single type of collective escape (but see [18,19,29] for work relating to fish schools). Overall, aerial displays in which several patterns of collective escape successively occur and overlap, like in the large murmurations of starlings, have never been investigated.

In the present paper, we examine the mechanisms underlying several patterns of collective escape in starlings, bridging the gap between empirical observations and theory. We assemble a dataset of flocks in the field by employing a bio-hybrid solution[30]: we record video footage of starlings under attack by a remotely-controlled robotic predator, the RobotFalcon[31]. From our empirical data, we learn that more than one pattern of collective escape arises sometimes simultaneously in a single flock. To study the emergence of such 'co-occurrence', we develop a biologically inspired 3-dimensional computational model of collective motion and escape specifically for starlings, through pattern-oriented modeling[32]. We simulate flocks of up to a few thousands of individuals under attack and identify the conditions at which different patterns emerge. We further show that hysteresis may underlie the density and shape dynamics of a flock, i.e., its current state is affected by its previous state[17,33].

Results

Collective escape of starling flocks

The RobotFalcon pursued starling flocks of around 20 to 2000 individuals for approximately 20 seconds to 2 minutes (with average pursuit duration of 1 min). Flocks were stationary in an open field and became airborne when noticed the RobotFalcon approaching. Video footage of the pursuit was recorded by a ground camera that followed the flock, and a camera on top of the robot (see supplementary Fig.1 for screenshots of both camera views).

The following patterns of collective escape arose in our empirical data: the collective turn (Fig. 1A), the split (supplementary Fig. S2), the cordon, the flash expansion, the agitation wave, blackening, compacting (supplementary Fig. S3) and dilution (supplementary Vid. S5). Starlings also executed 'columnar flocking': their flocks often took a vertical shape, elongated in altitude (Fig. 1B, supplementary Vid. S2B), something previously defined only in flocks of dunlins (*Calidris alpina*)[34,35]. More than one pattern of collective escape sometimes arose simultaneously in a single flock (Fig. 1B): the patterns 'co-occurred'. Collective turns most often co-occurred with the split, the columnar flocking, or the compacting (Fig. 1C). Flash expansions often appeared in the periphery of the flock where the RobotFalcon attacked, while at the same time in another part of the flock a collective turn or compacting was taking place. Agitation waves were observed only in the largest flock in our dataset. Since the emergence of agitation waves and flash expansions have been studied before[8,9,12,28], we focused our analysis on the other patterns. Most patterns can be seen in the supplementary Vid. S1, and a simplified schematic representation of part of its escape sequence is given in Fig. 1D, where we observe that parts of the flock behave differently.

At the individual level, we observed starlings evading the predator by performing level-turns (reverting their flight direction without large changes in altitude, Fig. 1A), dives (changing their altitude away from the predator, Fig. 1B), and diving turns (turning while diving, Fig. 1D). All maneuvers are marked in example footage in supplementary Vid. S2. We combined these observations with previous knowledge on the collective motion of starlings[20,23,26] to develop a new computational model to study their collective escape.

StarEscape: an agent-based model of starling flocks

We built a spatially-explicit agent-based model based on self-organization to simulate the collective escape of starlings, named *StarEscape*. The model consists of two types of agents: 'sturnoids' that form flocks, and 'predoids' that chase them (inspired by the 'boids' of Reynolds 1987[22]). Agents move in a large 3-dimensional space (effectively infinite). They are characterized by a position and a velocity vector in the global coordinate system, and their headings define the local coordinate system through which an agent senses the position and heading of its surrounding agents. Sturnoids have a set of 7 nearest neighbors (topological)[36] with which they interact through attraction, repulsion and alignment. Predoids follow the flock from behind for a given time period and then accelerate to attack towards a single sturnoid (target), similar to the strategy of the RobotFalcon in the field. Agents `update' their information about their surroundings with a limited 'reaction' frequency in an asynchronous manner, capturing the cognitive abilities of animals that cannot instantaneously react to one another in the speed of a simulation time step.

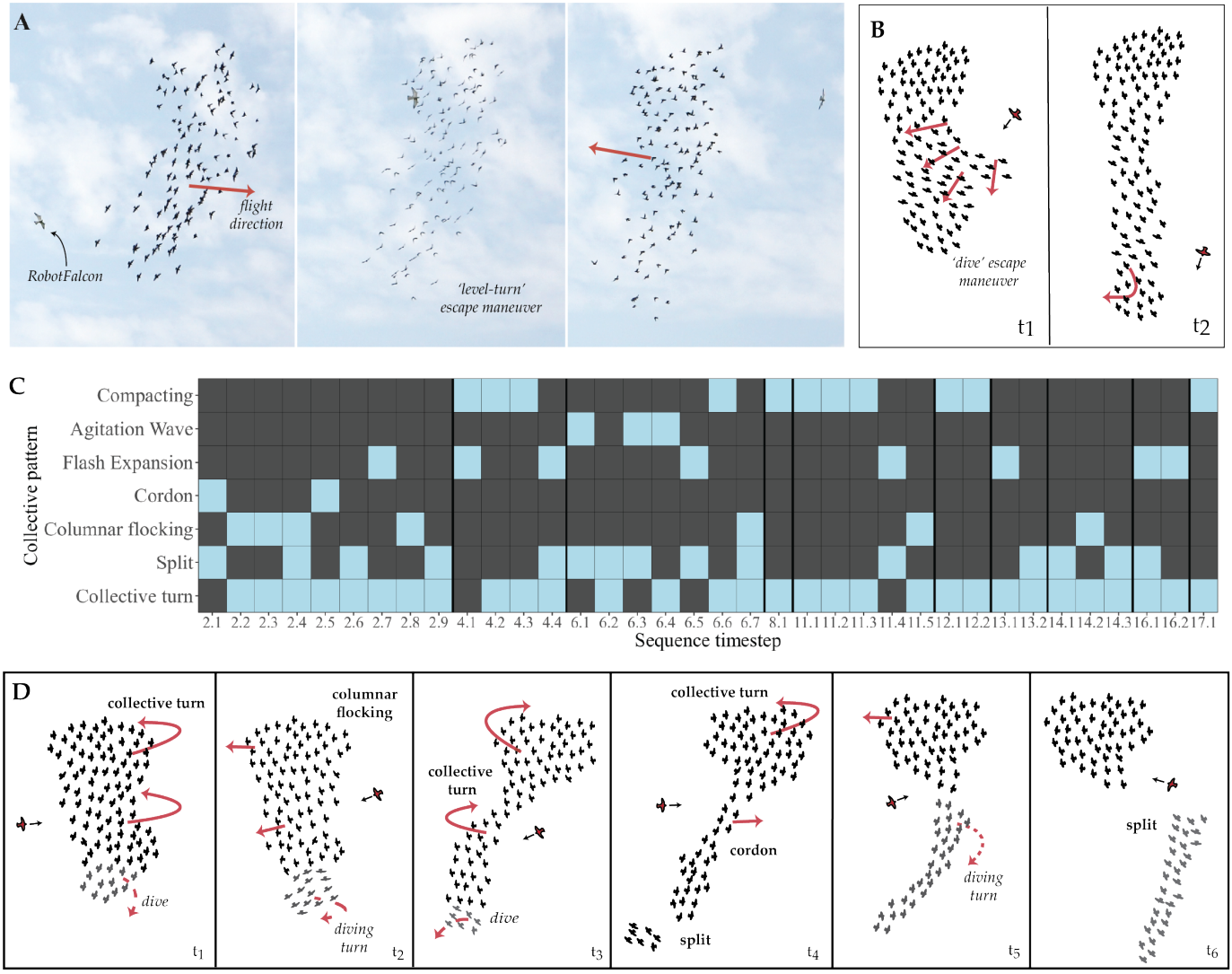

Figure 1. Empirical data of collective escape of starling flocks under attack by the RobotFalcon. (A) Screenshots of a flock performing a collective turn away from the RobotFalcon. Individuals perform a level-turn to evade the predator. The red arrows represent the flight direction of the flock. **(B)** Schematic representation of data of supplementary Vid. S2B: individual starlings (small birds in black) dive away from the RobotFalcon (larger bird in red, with black arrow showing its heading). How much individuals dive seems to relate to their distance to the predator. A columnar shape of the flock emerges. **(C)** Co-occurrence of collective patterns in the empirical data. Every timestep (2.1 – 17.1) corresponds to a small time-window in which certain patterns (light colored blocks) co-occur in a given flock (IDs 2, 4, 6, 8, 11, 12, 13, 14, 16, 17). **(D)** Co-occurrence of different patterns of collective escape (supplementary Vid. S1) where subgroups (parts of the flock) behave differently. Each window (t_1-t_6) represents a snapshot during the sequence of collective escape. The initial configuration of the flock and relative position to the predator are given at t_1. At t_2, individuals that form the main part of the flock have performed a collective turn in the opposite direction (approx. 180°), while a small number of individuals at the bottom of the flock dived. At t_3, individuals in the top part of the flock continue turning in the same direction, the ones in the middle part (closer to the predator) move slightly downwards (accelerating), while individuals at the bottom perform a diving turn. At t_4, the main flock has performed a collective turn (approx. 180°). Due to the elongation of the flock, a cordon is formed. Individuals in the bottom part of the flock do not turn and continue to dive; as a result, they split from the main flock. At t_5, individuals in the top part of the flock have performed another collective turn. Individuals in the middle and lower part continue their forward motion. At t_6, the top part of the flock continues its forward motion while the bottom part performs a diving turn. As a result, the flock splits in two.

Coordination rules and parameterization are adjusted to empirical data of starlings (see Methods for details). The individual behavior of sturnoids is split into 4 conceptual states: *flocking, alarmed flocking, escape,* and *refraction*. Transitions between the states are controlled by an individual-based and dynamic (non-homogeneous) Markov-chain. Overall, individuals just coordinate with their neighbors when the predator is far away (*flocking*), and switch to *alarmed flocking* when the predator gets closer, during which they increase their reaction frequency, resembling vigilace[37–39]. An individual decides to perform an escape maneuver based on a probability that depends on its 'stress' level (based on its distance to the predoid, see Methods), and its neighbors copy its escape. After the escape is complete, individuals cannot perform another escape maneuver for a few seconds (*refraction*). Sturnoids may perform two escape maneuvers, similar to the ones we observed in the starling flocks: level turns or dives.

We analyzed simulated flocks of 20-2000 sturnoids (see supplementary Vid. S3, S4, S6, and S7). The simulated flocks resemble flocks of starlings in their average speed (9.5 ± 0.32 m/s), nearest neighbor distance (NND = 0.86 ± 0.08 m, Fig. 2A) and stability of neighbors over a 3 seconds time window ($Q_4(3s)$ = 0.58 ± 0.06, Fig. 2B); values that are within the measured ranges for flocks of starlings in Rome (speed: from 6.9 to 15 m/s; NND: 0.68 – 1.51 m)[2,14,23]. The variability of flock shape in our model when uninterrupted by a predator is also qualitatively similar to real flocks (Fig. 2C).

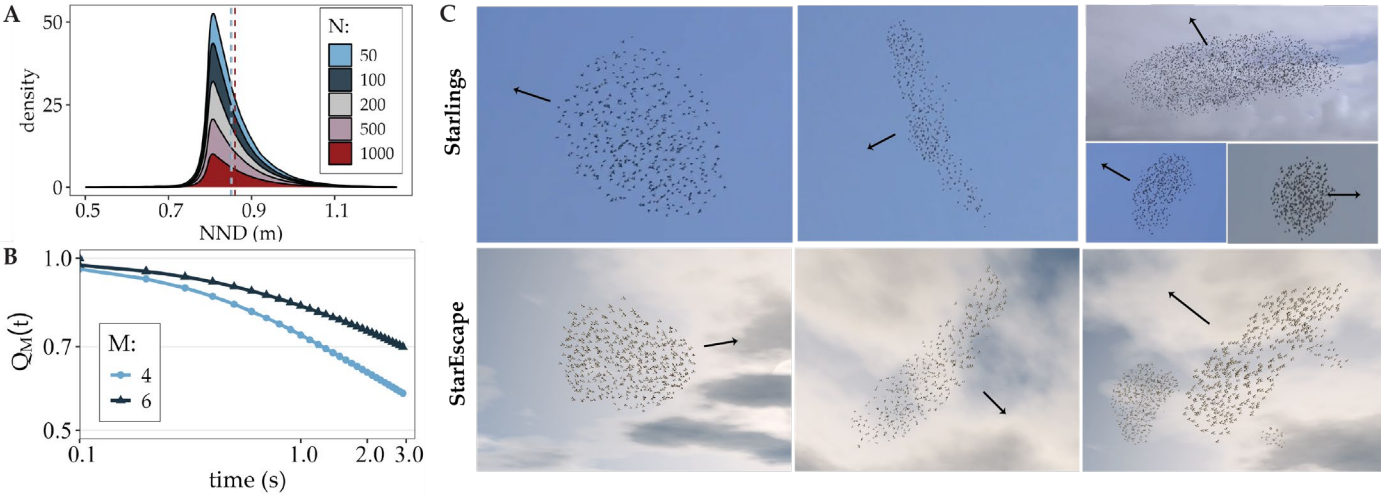

Figure 2. Flocking in StarEscape. (A) Distributions of nearest neighbor distance (NND) of simulated flocks of different sizes (N = 50-1000). The vertical lines indicate the average density (NND) for flocks of 50, 200, and 1000 individuals. **(B)** The average stability of neighbors (Q_M) for the closest 4 and 6 (M) neighbors over time in the simulated flocks. The timeseries of both NND and Q_M are exported by the model. **(C)** Flocks of different sizes and shapes in starling flocks (top row) and the StarEscape model (bottom row). The arrows show the direction of motion of the flock.

The emergence of collective patterns

Several patterns of collective escape emerged from sturnoids performing level-turning and diving maneuvers (Fig. 3). Interestingly, sturnoids also performed diving-turns in the model (without them being explicitly modelled) when reacting to the predoid with a turn before leveling their pitch after a previous diving maneuver (see supplementary Fig. S4). Compacting emerged in our model from the flock becoming alarmed (with more frequent interactions among individuals), as a response to increased stress when the predoid was approaching (supplementary Fig. S5).

In our simulations the whole flock often turned collectively, propagating from a single or a few initiators with similar relative positions to the predator (Fig. 3A, supplementary Vid. S3). Splits of sub-flocks emerged when part of a flock was performing a collective turn and the other flock members did not follow (Fig. 3B), i.e., when the level-turn did not propagate fast enough through the group. A split emerged also when two initiators turned in opposite directions, being each followed by their own subset of neighbors (Fig. 3B-3C). This happened particularly when the predator approached from behind the middle of a flock, resulting in the two halves of the flock having different escape directions. Thus, sub-flock splits almost always co-occur with one or several collective turns. Due to the copying mechanism, singletons rarely split off, and when they did it was from the periphery of large flocks. During sharp escape maneuvers, blackening, compacting, and collective turn co-occurred (Fig. 3C). Blackening during collective turning may relate to both the relative orientation of the flock and the observer, and to an increase in group density.

Diving maneuvers usually led to columnar flocking and cordons (Fig. 3D-3E). Since the diving tendency of each individual increases when it is closer to the predator, columnar flocks emerged when the tendency of a flock member to dive resembles that of its neighbors, i.e., when the predator is at a similar distance from all prey as in spherical flocks (Fig. 2C). If the predator approaches the lower half of the flock, a dive may propagate only to that lower part of the flock (supplementary Fig. S6). In this case, since flock members were still coordinating, there were a few individuals in the middle that were influenced by the position and heading of the diving individuals but did not dive themselves. As a result, these individuals, along with the top individuals of the diving subgroup, formed a 'cordon', connecting the two larger parts of the flock (Fig. 3E). If the predator performed a fast attack at the bottom of the flock, a sub-flock split off, because a small number of individuals were rapidly diving and there was not enough time for the dive to propagate to the rest of the flock. Collective turns while in columnar flocking, as observed in our empirical data (Fig. 1D and supplementary Vid. S1), also emerged in StarEscape (supplementary Vid. S4).

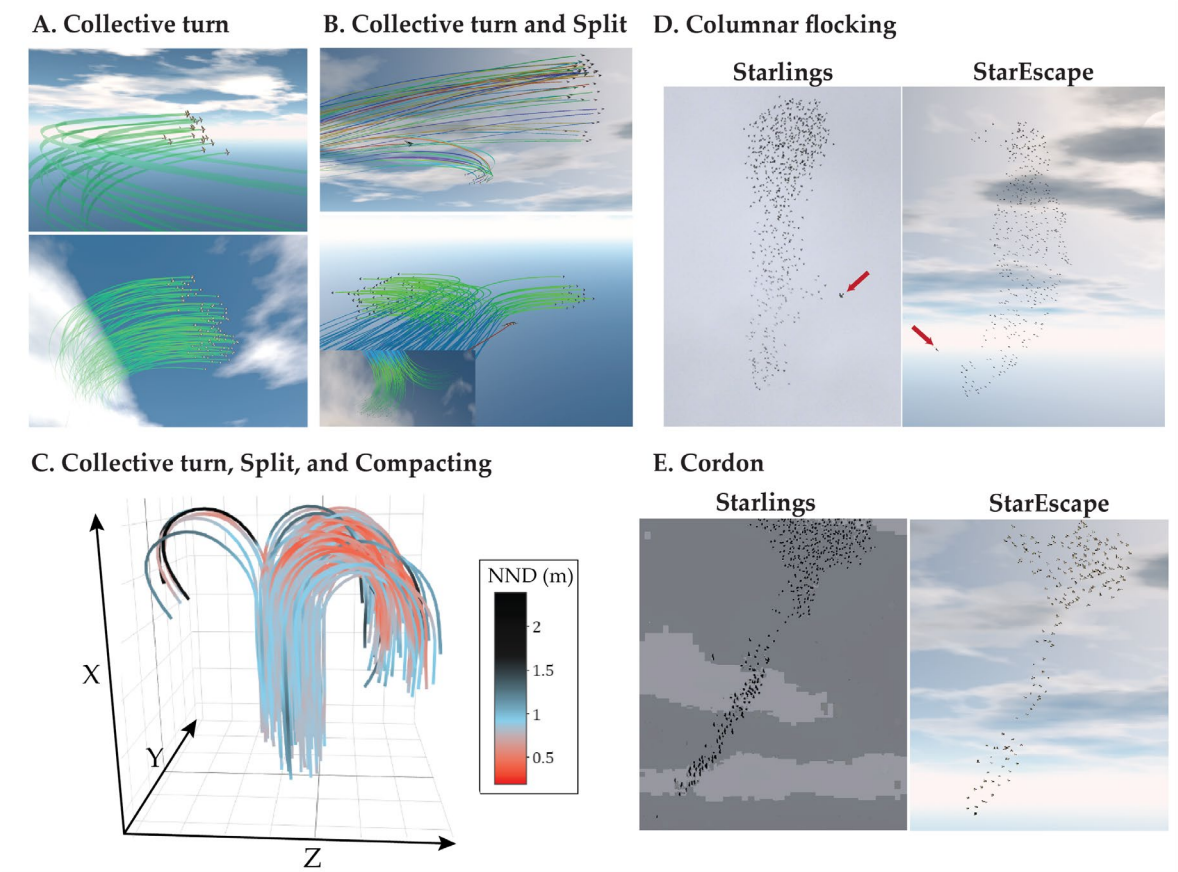

Figure 3. Patterns of collective escape in StarEscape. (A) Collective turns in flocks of 20 (top) and 200 (bottom) individuals, often co-occurring with **(B)** splits, and **(C)** compacting, emerging form individual level-turns. The trajectories and timeseries of nearest neighbor distance (m) shown in (C) are exported by the model at the end of a simulation (N = 200). Altitude varies along the y-axis. From diving maneuvers, **(D)** columnar flocking and **(E)** the cordon emerge, similarly to what is observed in flocks of starlings pursued by the RobotFalcon. The red arrows in (D) indicate the position and orientation of the RobotFalcon and predoid (attacking a flock of 500 sturnoids).

Hysteresis

Expansion and compression of the flock emerged through hysteresis: during a collective turn the flock often became denser, leading to a decrease in density right after the evasion and before returning to its regular density (Fig. 4A-C). This emerges despite the rules of interaction and the parameterization of the 'alarmed flocking' behavior being identical before and after a collective turn (Fig. 4B). The dynamics of this initial compacting may be linked to the differences in the timing of turning across group members (supplementary Fig. S7), making individuals decrease their nearest neighbor distance during the turn and avoidance interactions being stronger after.

Apart from these dynamics of collective motion during evasion, the pattern of dilution in our model also emerged by hysteresis. It occurred as a side-effect of flock-members decreasing their reaction frequency when switching from alarmed flocking to regular flocking when the predoid retreated (supplementary Vid. S5). Just from this change in coordination frequency, and with a denser flock pre-existing, the flock dilutes, taking a shape that differed from its shape at the initial condition before the predator's attack (Fig. 4D). This matches the empirical observation that starling flocks dilute when they move away from the predator (Fig. 4D, supplementary Vid. S5).

Discussion

The first model of collective escape in swarms, namely fish schools, was published more than 20 years ago[18]. To date, the complexity of the collective escape of starlings still makes their understanding particularly challenging. Overall, our results show that the diversity of aerial displays of starlings under predation arise from a combination of (1) some individuals start performing an escape maneuver, (2) the speed with which this information transfers through the flock, (3) the local conditions of each flock member (i.e., its position in the flock and its relative position to the predator) that determines its exact reaction, and (4) the relation between patterns (group shape and density) through time, i.e., hysteresis. To better understand how the diversity of patterns of collective escape of large flocks emerge in nature, future research should focus on these elements.

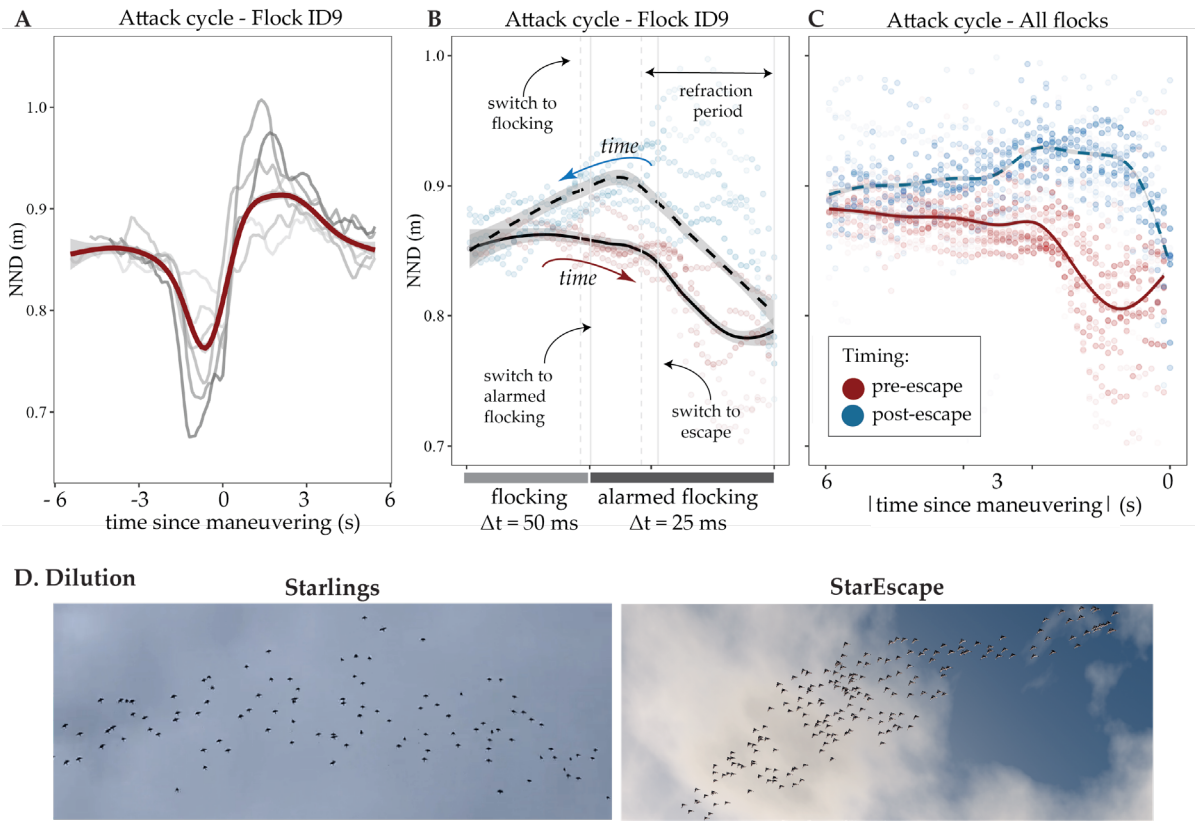

Figure 4. Hysteresis in collective escape. (A) Average nearest neighbor distance (NND) during an attack cycle of a simulated flock. Time 0 is the end of a turning escape maneuver. Grey lines show the time series of average NND during individual collective turns across the pursuit sequence. **(B-C)** The time series over absolute time relative to the end of an escape maneuver. The solid lines mark the decrease in NND as flock members transition from regular to alarmed flocking (decreasing their reaction time from 50 to 20 ms), and then start performing an escape maneuver ('pre-escape' period). The dashed lines show the return to regular flocking (post-escape), during which flock members have the same reaction frequency but higher NND as a result of the previous compacted state of the flock. The points show the average NND of a flock at each given point in an attack cycle. The vertical solid and dashed lines in (B) indicate the points that all group members have switched to a given state. **(D)** The pattern of dilution emerges when individuals decrease their reaction frequency (switching from alarmed flocking to flocking) after the predator's attack. Examples of dilution at the end of pursuits are also given in supplementary Vid. S3 and S5.

How the geometry of the group affects the dynamics of collective escape or decision-making[40] has rarely been studied, despite affecting many group properties. An example of this is the columnar flocking we observed here. While the flock is columnar rather than spherical, the large differences in the relative position of individuals to the predator and the increased distance of all group members to the center of the flock cause turning information to take longer to propagate from one edge of the flock to the other[41]. As a consequence, when collective turns co-occur with columnar flocking, a cordon or a split may emerge, depending on the position and angular velocity of the escape initiator[13]. The cordon tends to also lead to the split, since the two large parts of the flock experience different threat levels due to their different relative positions to the predator. It is interesting to note that the expected hunting strategy of predators of attacking the less dense part of a group (which during this formation is the cordon) to decrease confusion effects[35,42,43], also enhances splitting, which may further benefit the predator[44].

The specifics of escape maneuvers, information transfer, and local conditions we uncover here are valuable to also understand the emergence of other collective patterns of starlings, such as the agitation wave[11,45], the flash expansion[8,12] and the vacuole[8]. The agitation wave can emerge from a zig-zag maneuver: individuals sequentially turning slightly to the left and then to the right (or vice-versa)[9]. Concerning the specifics of information transfer, previous work on agitation waves showed that more realistic waves (damping) emerge if individuals copy their neighbors' maneuver with the same probability, but perform a less extreme maneuver (i.e., reduced banking) when they are further away from the predator[28]. 'Vertical' compacting in starlings, a fast compression of the flock from the top that has never been studied, may emerge from a similar mechanism: the reduced copying of a diving maneuver and the predator attacking the flock from the top. Understanding such propagation mechanisms is also important for wave propagation in other systems (e.g., sulphur mollies under attack by avian predators[46,47]). The flash expansion can emerge from a fast turning maneuver away from the predator[12,48]. According to our empirical observations and to previous findings in whirligig beetles[48], the flash expansion is a very localized pattern, emerging as a direct response away from the position of the predator when the predator gets very close to some individuals at the edge of a large flock. The vacuole, a rare pattern seen only in very large flocks of starlings, is common in

fish schools[10,18] where the group speed is slower and predators less maneuverable[19]. The fact that both patterns are characterized by the prey being close (but not too close) to the predator without trying to escape when in large groups, may be due to the dilution effect: individuals have a higher tendency to stay in the group[49] and can save energetic costs of maneuvering, until the threat is too high. To better understand the emergence of more complex aerial displays, detailed information about escape reactions of prey individuals in relation to the predator's position and speed[50–56], as well as their flock mates' reactions, is necessary.

Our results further highlight that hysteresis may be crucial in the emergence of complex aerial displays. In collective motion of fish-like agents, a single parameter combination is shown to lead to both milling and polarized motion, depending on whether the behavior of the group before was ordered or disordered[17]. We showed that a single parameter combination can lead to both a spherical compacted flock, and a wide, diluted flock (lower density), depending on whether the flock has been compacted or loose before. In self-assembling army ants, hysteresis has been identified when the gap that their bridge is covering is decreasing, with more individuals composing a bridge over the same distance than when the gap was increasing[33]. In starlings, the effect of hysteresis we identified also relates to the fast sequence of 'unstable' states of the flock during the whole sequence of a pursuit, while the flock transitions from noticing a predator, to escaping, and relaxing after the predator retreats. This temporal aspect of hysteresis ('short-term' hysteresis) has never been studied before and may play a crucial role in the emergence of complex starling murmurations, emphasizing the importance of considering long behavioral sequences in studies of collective escape.

At the individual level, one aspect of behavior that is affected by the presence of the predator is the specifics of social interactions among prey, as known for fish schools[37]. However, changes in the vigilance level of individuals, captured in agent-based models by the update or reaction frequency of each group member, has also been shown to lead to fast accelerations[57] (as identified in empirical data[37]) and changes in the internal structure of the group (diffusion)[24], without changes in the actual rules of social interactions. Our *StarEscape* simulations show that changes in the reaction frequency of group members may also underlie an emergent decrease in density, in line with what was expected to arise from the selfish herd hypothesis[4,49], but without an explicit increase in the tendency of individuals to move towards the center of their flock. This highlights the importance of considering such fine-scale effects of self-organization when interpreting collective phenomena.

Most of our current understanding of how patterns of collective escape emerge comes from studies on fish schools[18,19]. However, there are large differences between the locomotion type and evasive maneuvers of fish and birds, and in the internal structure of their swarms[27,58]. Detailed investigation on how rules of interaction and escape 'translate' across systems is essential before it is useful to generalize findings. Therefore, we cannot assume that the same mechanisms as in fish[18,19,29] underly patterns of collective escape in starling flocks. A limiting aspect of most existing models is their 2-dimensions, given the complex 3-dimentional structure of starling flocks under attack. Concerning this, for example, our empirical data, combining footage from the ground camera and the RobotFalcon (see supplementary Fig. S1), show that compacting co-occurring with collective turns can also be an effect of the observer's orientation[9,29] .

StarEscape is a valuable tool to study the complex aerial displays of bird flocks in more detail in the future. The user interface, simulation speed, and its detailed output facilitate its future use (supplementary Fig. S9). In our simulations, a sturnoid selects which escape maneuver to perform stochastically, according to a parameterized probability. However, we also included a biologically relevant functionality: the probability of selecting each maneuver can also depend on the local information of each sturnoid, such as its relative position to the predator or flock mates, or the predator's speed. For instance, when the predator is diving on the flock in high speed or the attacked individual is at the bottom of the flock, choosing a diving maneuver may be advantageous. Since empirical data to inform such individual decision-making is not yet available, this functionality is not used in the simulations presented in this paper.

An important aspect for future studies is to investigate in detail the effect of the position of the initiators and the predator on the frequency of each pattern across the parameter space of our model. To achieve that, an important challenge to overcome is the automated identification of the different patterns, i.e., a quantitative definition of each type of collective escape, similar to distance-based thresholds used for splitting in pigeons[13] and proxy metrics used to study patterns of collective motion such as turning[24] and milling[25]. Apart from this process-oriented investigation, a function-oriented analysis in our model can show the adaptive advantages of different patterns, how they affect the catching success of the predator[43]. *StarEscape* can further be adjusted to other bird species, such as dunlins[35], since the coloration and shape of agents in our model can be changed (see supplementary Vid. S6), allowing across species comparisons[29,58]. For instance, the 'rippling' effect that dunlin flocks demonstrate[35] may be the result of orientation waves similar to the ones of starlings[9,35]. Overall, studying the relation among several patterns of collective escape in bird flocks (instead of treating them as independent snapshots) is necessary to improve our understanding of starling murmurations, and complex aerial displays in general.

Methods

Data acquisition

We qualitatively analyzed video footage of flocks of European starlings (*Sturnus vulgaris*) pursued by our RobotFalcon[31]. The RobotFalcon is a remotely controlled aerial predator that resembles a peregrine falcon (*Falco peregrinus*) in appearance and size. It is steered by a trained pilot, aiming to imitate the hunting behavior of the real falcon. The pilot has a first-person view of the flock through a camera mounted on the back of the RobotFalcon (supplementary Fig. S1). The RobotFalcon approached the flock from a distance while the flock was on the ground and continued to an aerial pursuit when the flock took off, until it left the site. The dataset was collected between February and November 2019 at agricultural sites in the north of the Netherlands (52°59'N- 5°27'E).

Empirical data analysis

In the footage, we identified the patterns of collective escape according to previous classifications[7,8], with the exception of the split. We identified a split when part of the flock formed a new cohesive flock, without taking into account splits of one or a few individuals (as a result of a flash expansion for instance, as done in previous work of small groups of 10-30 individuals)[13,15]. We further recorded whether in a single flock different patterns of collective behavior were exhibited simultaneously. In detail, we analyzed videos of approximately 15 minutes of pursuit by the RobotFalcon using the Adobe Premier Pro software. We factorized each video into a sequence of steps during which a new collective state is observed. In addition, for each event of collective escape, we examined the motion of individual starlings, particularly focusing on changes in their heading and altitude. We further selected few visible individuals close to the point of attack of the RobotFalcon and tracked their motion. We used our observations to develop a computational model.

A computational model of collective escape

We built an agent-based model to simulate the collective escape of starlings (*StarEscape)*. The model is based on the principles of self-organization with two types of agents moving in an open 3-dimensional space: 'sturnoids' that coordinate with each other and 'predoids' that pursue and attack the sturnoid flocks. A detailed model description is given below, using elements of the ODD protocol[59]. The model is written in C++, using OpenGL for the real-time visualization of the simulation, and DearImGui for the graphic user interface (GUI, supplementary Fig. S9). Many agent variables such as the speed, nearest neighbor distance, state, and flock id of each individual can be monitored in real time through the GUI. All parameters mentioned below are given in the supplementary Table S1.

Model overview

All agents are defined by a position and a velocity vector in the global coordinate system. The heading of each agent defines its local coordinate system (Fig. 5A) through which an agent senses the position and heading of its interacting agents. Sturnoids have a set of nearest neighbors with which they interact (set $\mathbb{N}$) and predoids have a flock or a sturnoid as a target. According to empirical findings on starling flocks, we model topological interactions between individuals[36]. Each sturnoid interacts with its 7 closest neighbors (N_{topo}) that are within its field of view (θ_{FoV}) according to the rules of alignment, attraction and avoidance (*flocking sub-model*[59]).

Apart from their neighbors, sturnoids sense the position of the closest predoid and their 'alertness' (or 'stress') increases as they get close to it (Fig. 5B). Sturnoids react to the predoid with an evasive maneuver based on a probability that depends on their alertness (similar to decision-making processes in models of evidence accumulation in social systems[60]). The neighbors of an escaping sturnoid copy its maneuver. A predoid first chooses a flock and follows it from a given point relative to its center (based on the parameters β_{at} and d_{at}). From there, it picks its closest sturnoid as its target and attacks it. The attack has a specific duration after which the predator gets re-positioned far away from the flock. Since we focus on the emergence of collective escape patterns, we do not model 'catches' of sturnoids by the predator.

Behavioral states

The individual-level rules of motion and interaction in our model depend on the 'state' of each agent. For sturnoids, we define 3 behavioral states: a coordination state, an alarmed-coordination state, and an escaping state (Fig. 5C). An individual-based non-homogeneous Markov Chain controls the transition from one state to another. The transition probabilities depend on the alertness of each individual at each timestep, which depends on its distance to the predator. When a sturnoid is close to the predator, its alertness increases every time it updates its information about the predator's position, according to a given function (see section 'Escape' and Fig. 5B, the closer the predator the higher the increase of alertness), and decays with a constant rate (r_{decay}). The increase and decay of alertness is balanced in order for alertness to always increase when the predator is close and decrease back to 0 within a few seconds after the predator retreats. From this mechanism, indi-

viduals switch to alarmed coordination (higher reaction frequency) when the predator starts pursuing the flock, spontaneously escape (depending on alertness) when it gets close, and return to their basic coordination when the predator stops its pursuit.

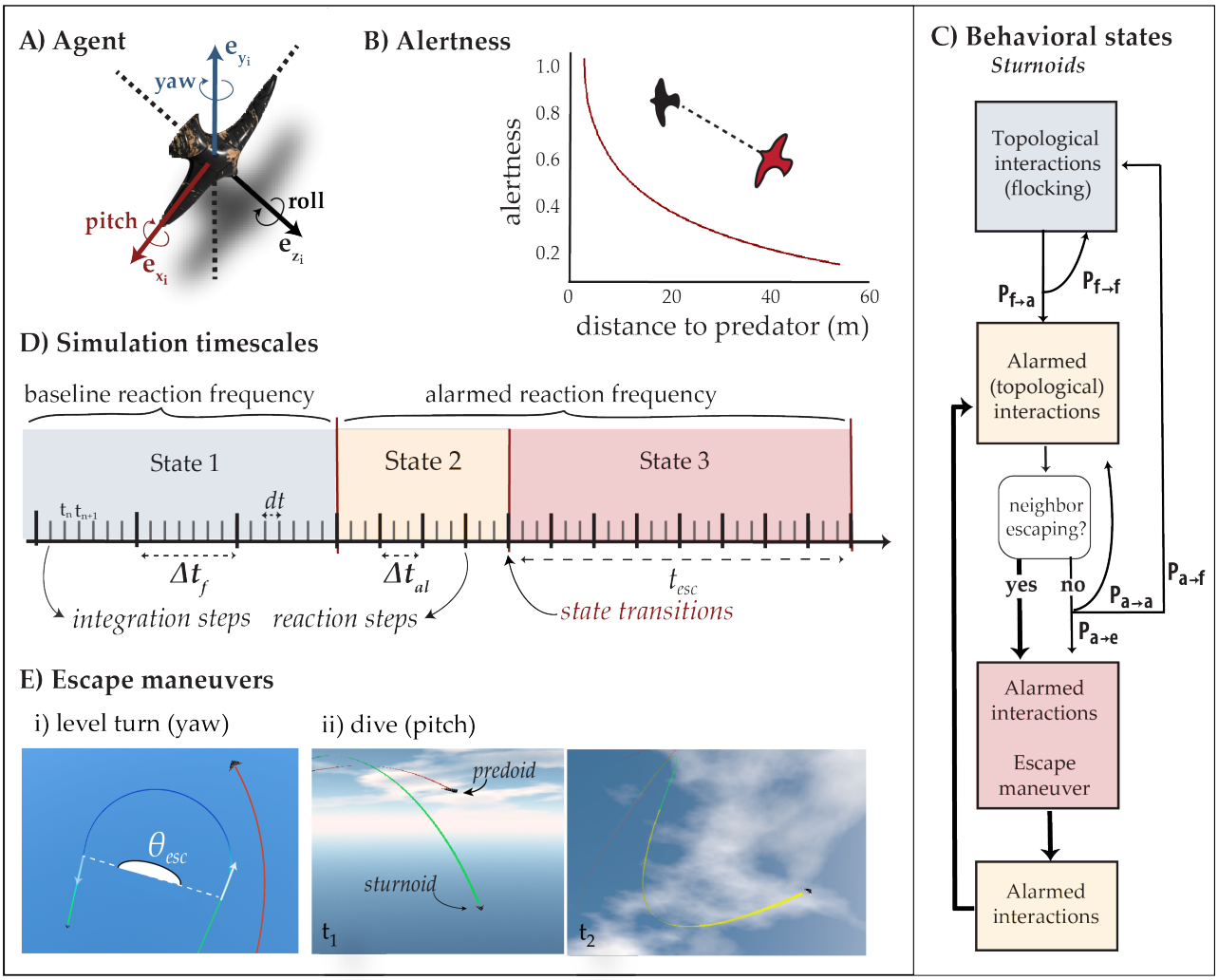

Figure 5: **The StarEscape model. (A) The local coordinate system of an agent in the 3-dimensional space.** The vectors e_x, e_z, and e_y represent the sideward, forward, and upward directions of the agent, respectively. The agent yaws and rolls to turn, and pitches to dive or climb. **(B) Alertness increase.** The alertness of each individual accumulates at each update timestep as a function of its distance to the predator. **(C) The transition mechanism between behavioral states in sturnoids**. The transition probabilities ($P_{x\text{->}x}$) represent the dynamic Markov-chain of each individual and thicker arrows represent deterministic transitions. In detail, sturnoids may transition from their regular coordination (with update frequency $1/\Delta t_f$) to an alarmed state if their alertness increases. During alarmed coordination, their coordination frequency ($1/\Delta t_a$) is increased and a sturnoid may perform an escape maneuver based on its probability to escape or copy the escape of its neighbors (transitioning to an escape state). Each escape has a predefined duration (t_{esc}), after which agents transition back to alarmed coordination without the option to perform an escape maneuver (refractory state). After this, they regain the probability to react to the predator and the cycle starts again. If alertness decreases, individuals transition back to regular coordination. The exact values of the Markov chain depend on each individual's alertness. We derive them by interpolating through 3 parameterized transition matrices for low, intermediate, and high alertness. The chain of the predoid is given in supplementary Fig. S8. **(D) The timescales of StarEscape.** At every integration step (t_n) individuals update their position and heading according to their steering force (with frequency $1/dt$). At every reaction step, individuals recalculate their steering force, representing the cognitive collection and processing of information from their environment (with frequency $1/\Delta t$). At these time steps, each individual also decides whether to stay in its current state or switch, depending on its Markov-chain. **(E) Screenshots of the escape maneuvers of individual sturnoids in a simulation.** Sturnoids escape the predator by two evasive motions, (i) a level turn (with angular change θ_{esc}) or (ii) a dive (t_1, after which they return to level flight, t_2). The blue and green tracks show the sturnoids' trajectories during escape, the red tracks show the predoid's trajectories, and the yellow track the refractory period and pitch recovery after the diving maneuver.

During coordination, group members align with, are attracted to, and avoid each other (for details see section 'Coordination'). Sturnoids are also attracted to their roost and to a given altitude (see section 'Physics of motion'). During alarmed coordination, individuals coordinate with each other more often (higher reaction frequency, Δt_a), according to empirical evidence that prey individuals have faster reactions under predation (more frequent interactions with neighbors)[37,57]. When alarmed, individuals may switch to an escape state. This switch is either an individual 'decision' (based on the probability of their Markov chain) or induced by an escaping neighbor; individuals copy the escape reactions of their neighbors

(n^{topo}_{copy}). During escape, sturnoids perform an evasive maneuver while coordinating, with the relative influence of each term (e.g., alignment, attraction, turn away) being controlled by their relative weights. After escaping, individuals return to an alarmed-coordination state without the possibility to escape for a specific period of time (conceptualized as a refractory period, t_{ref}). This chain of behavioral states and its transitions are given in Fig. 5C.

The predoid in our simulation has 3 behavioral states. First, it perceives the largest flock (in case a split has occurred) and positions behind it at a given distance (d_{at}) and bearing angle (on the horizontal and vertical plane, β_{at}) from the flock's center and velocity, adopting its heading (*preparation state*). Second, it follows the flock ('shadowing') or locks into its closest sturnoid and moves towards it, with a speed that scales from the target's speed (u_{scale}, e.g., 1.3 times faster than the sturnoid; *attack state*). Third, after the attack duration has passed (t_{hunt}), the predator repositions away from the flock for a given time period (*retreat state,* $t_{retreat}$). The cycle then repeats, and a new attack takes place. Thus, all the states of the predoid (see supplementary Fig. S8) have predefined durations, like the refractory period of sturnoids and opposite to the rest of the sturnoids' states that spontaneously alternate.

We further describe the sub-modules of each state below. To better understand their specifics, we first explain the behavioural timescales in our model and how individual motion is controlled.

Timing

In the model, time is measured in seconds according to a parameter that scales a time step of the model to the real units of time (*dt)*. We use two timescales, the 'integration step' and the 'reaction step'. A single time step (*dt* seconds) is an 'integration' step. Since individuals cannot instantaneously receive, process, and react to information about their environment, we define as 'reaction step' the frequency with which individuals update their information about their environment (neighbors and predator). Every reaction step consists of several integration steps, during which agents integrate the information they collected in the preceding reaction step by adjusting their position and heading (Fig. 5D). Since grouping individuals in nature are not perfectly synchronized, individuals in the model update their information asynchronously (at different integration steps) but with the same frequency. During a reaction step, individuals may also switch state as described above.

'Physics' of motion

Individuals are steered in the global space by a pseudo-force (referred to as 'steering force'): a 3-dimensional vector that pushes individuals to their future position and heading. The steering force has 4 components: 1) a coordination force, 2) an escape force (for sturnoids) and a hunting force (for predoids), 3) a control force, and 4) a drag force. Large values in the forward direction (z) of the steering force will make individuals accelerate, towards the side (x) will make them turn, and in the vertical direction (y) will make them change altitude (dive or climb). The steering force is calculated at each reaction step and applied at each integration step to determine the new position and heading of each agent.

The coordination and escape forces are explained in the next sections. The drag force keeps individuals around a predefined speed ('cruise speed', u), given that birds have a preferred speed from which they cannot deviate for long. Thus, 'drag' in our model is a spring force: the more an agent deviates from its cruise speed, the more it is pulled back to it (with weighting factor w_u). The control force represents the inability of birds to climb sharply (especially when they are part of a flock). We constrained the pitch of an individual to a given maximum (p_{alt}). We also model an 'altitude attraction': individuals have a preferred altitude (y_{alt}) towards which they tend to return according to a smootherstep function[61]:

$$\psi_i^{alt} = w_{alt}\,\xi(-1 + 2 \times \begin{cases} 0), & if\ d_i^{alt} = 0 \\ 6x^5 - 15x^4 + 10x^3), & if\ 0 < |d_i^{alt}| \le \sigma_{alt} \\ 1), & if\ \sigma^{alt} < |d_i^{alt}| \end{cases} \qquad \textit{Altitude attraction (1)}$$

where $x = \frac{d_i^{alt}}{\sigma_{alt}}$, σ_{alt} is the smoothing parameter around the preferred altitude, w_{alt} the weighting factor of altitude attraction, $\xi = -sin\ (p_{alt})$, with p_{alt} the maximum pitch for altitude attraction (in rads), and $|d^{alt}{}_i|$ the absolute deviation of the altitude of individual i from the preferred altitude. To keep our flocks within our simulation space, we define a 'roost' inspired by real flocks[7,14,20]. It is a point towards which sturnoids are attracted (with weighting factor w_r) if they get far away from it (outside a radius θ_r around it). It is important to note that the control force is not active during escape; we assume that an individual prioritizes escape over attraction to its roost and minimization of its energetic costs[52]. Similarly, there are no aerodynamic forces in our model[20]. For our agents to qualitatively resemble the flying motion of birds, we visualize agents with delta-shaped bodies, the coloration of starlings, and enforce a `banking' motion, i.e., individuals roll according to their turning rate[9,26].

Coordination

The specifics of coordination affect the motion of a sturnoid continuously. Attraction pulls each individual towards the center of its neighborhood ($n^{topo}{}_{coh}$). The strength of this force depends on the individual's distance to that center: the further away a sturnoid is from its neighbors' centroid, the stronger the force is. Alignment turns an individual towards the average heading of its neighbors ($n^{topo}{}_{ali}$). Avoidance makes the individual turn away from the position of its closest neighbor, if the neighbor is within a range of minimum separation (d_s). We parameterize each sturnoid to avoid only its closest neighbor (instead of their n^{topo} closest neighbors) for the diffusion of flock members in our simulations to resemble more empirical data of starlings[23]. Noise to each individual's motion is also added through a pseudo-force perpendicular to its heading with magnitude sampled from a uniform distribution with bounds $-w_n$ and w_n (weighting factor for random noise).

Escape

At every reaction step, the alertness of an individual accumulates according to the function $w_{stress} * e^{-\frac{\sqrt{d_i^p}}{\sigma_s}}$ (with d_i^p being the distance between the focal individual *i* and the predator, σ_s a scaling parameter, and w_{stress} the weighting factor for stress accumulation), and at every integration step it decays (with rate r_{decay}). The higher an individual's alertness is, the higher its probability of performing an escape maneuver. A set of probabilities assigned to each maneuver controls which evasive action the individual will perform. We investigate two maneuvers in our model: a level turn and a dive (Fig. 5E). During turns, individuals make a turn of θ_{esc} degrees (here $\simeq 180^o$) away from the predator (depending on their own heading relative to the predator's heading). During dives, individuals pitch downwards depending on their own distance to the predator (the closer the predator the steeper the dive). This distance dependency is controlled by a smootherstep function (similar to Eq. 1):

$$\psi_i^{dive} = w_d\,(-1 + \begin{cases} 0), & if\ d_i^p = 0 \\ 6x^5 - 15x^4 + 10x^3), & if\ 0 < d_i^p \leq \sigma_d \\ 1), & if\ \sigma_d < d_i^p \end{cases} \qquad \textit{Dive maneuver (2)}$$

where $x = \frac{d_i^p}{\sigma_d}$, w_d is the weighting factor for diving, and σ_d the smoothing parameter that denotes the minimum distance from the predator for a sturnoid to dive. When an individual exceeds a maximum dive distance (d_d), it starts pitching upwards to get to its preferred altitude. Note that during copying, an individual copies the type of escape maneuver from its neighbor (turn or dive), but bases the specifics of the maneuver on its own local conditions (relative position and heading to the predator). The topological range for copying ($n^{topo}{}_{copy}$) is set to the same value as for coordination.

Initialization, data collection, and experiments

Our simulations include a single predoid and many sturnoids (N <=5000). Sturnoids are initialized in a flocking formation: with a small heading deviation around a given global heading and positioned within a radius around a given point in space. This resembles the starting conditions of the starling flocks in our empirical experiment. The predator is initialized a few seconds after the flock and immediately enters its preparation state (positioned behind the flock with the same heading as its target). All parameter values (supplementary Table S1) are given to the compiled model through a configuration file (*.json*) at run time. We focus on which patterns emerge across simulations. A camera that follows the flock (with a certain flock member as its center) shows the simulation in real time. The user can move the orientation of the camera to look at the flock from a different perspective (see supplementary Fig. S9 and Vid. S7). We collected screenshots and recordings of the emerging patterns of collective escape across simulations. We compare these observations with the empirical, qualitative data of starlings' collective escape (video recordings).

A number of measurements are computed by the model in real time and exported at the end of each simulation. Specifically, the model exports data (in *.csv* format) concerning timeseries of individual motion and flock characteristics at a given sample frequency (f_s). The individual timeseries consist of position (x,y,z), heading (x,y,z), speed, acceleration (x,y,z), state, NND, relative position and direction to the flock's center. The flock characteristics include flock size, id (in case the flock is split), stability of neighbors, and volume (calculated based on an object-oriented bounding box that includes all flock members, as in [26]). The configuration file used for each simulation is also copied to the exported data folder. To assess the resemblance of collective motion in our model with that of starlings, we compared the average speed, nearest neighbor distance and stability of neighbors (based on the 4 and 6 closest ones, measured as in [2,23,24]) of our simulated flocks (N = 50-1000) with previously collected empirical data of starlings in Rome[2,14,20]. We further investigated the dynamics of these properties during collective escape, using trajectories from 20 simulations with 90 second pursuits (according to the average pursuit duration of the RobotFalcon) on flocks of 100-200 individuals. Data analysis and visualization was performed in R.

References

1. Landeau, L. & Terborgh, J. Oddity and the 'confusion effect' in predation. *Animal Behaviour* **34**, 1372–1380 (1986).
2. Cavagna, A., Queiros, S. M. D., Giardina, I., Stefanini, F. & Viale, M. Diffusion of individual birds in starling flocks. *Proceedings of the Royal Society B: Biological Sciences* **280**, 20122484–20122484 (2013).
3. Krause, J. & Ruxton, G. D. *Living in Groups*. (Oxford University Press, Oxford, UK, 2002).
4. Hamilton, W. D. Geometry for the selfish herd. *Journal of Theoretical Biology* **31**, 295–311 (1971).
5. King, A. J. & Sumpter, D. J. T. Murmurations. *Current Biology* **22**, 112–114 (2012).
6. Selous, E. *Thought Transference or What in Birds*. (New Science of Life: Hypothesis of Formative Causation, London, Paladin, London, 1931).
7. Carere, C. *et al.* Aerial flocking patterns of wintering starlings, Sturnus vulgaris, under different predation risk. *Animal Behaviour* **77**, 101–107 (2009).
8. Storms, R. F., Carere, C., Zoratto, F. & Hemelrijk, C. K. Complex collective motion: collective escape patterns of starling flocks under predation. *Behavioral Ecology and Sociobiology* **73**, (2019).
9. Hemelrijk, C. K., van Zuidam, L. & Hildenbrandt, H. What underlies waves of agitation in starling flocks. *Behavioral Ecology and Sociobiology* **69**, 755–764 (2015).
10. Parrish, J. K., Viscido, S. V. & Grünbaum, D. Self-organized fish schools: An examination of emergent properties. *Biological Bulletin* **202**, 296–305 (2002).
11. Procaccini, A. *et al.* Propagating waves in starling, Sturnus vulgaris, flocks under predation. *Animal Behaviour* **82**, 759–765 (2011).
12. Romey, W. L., Smith, A. L. & Buhl, J. Flash expansion and the repulsive herd. *Animal Behaviour* **110**, 171–178 (2015).
13. Papadopoulou, M., Hildenbrandt, H., Sankey, D. W. E., Portugal, S. J. & Hemelrijk, C. K. Emergence of splits and collective turns in pigeon flocks under predation. *Royal Society Open Science* 211898 (2022) doi:10.1098/rsos.211898.
14. Ballerini, M. *et al.* Empirical investigation of starling flocks: a benchmark study in collective animal behaviour. *Animal Behaviour* **76**, 201–215 (2008).
15. Sankey, D. W. E. *et al.* Absence of "selfish herd" dynamics in bird flocks under threat. *Current Biology* 1–7 (2021) doi:10.1016/j.cub.2021.05.009.
16. Aoki, I. A Simulation Study on the Schooling Mechanism in Fish. *Bulletin of the Japanese Society of Scientific Fisheries* **48(8)**, 1081–1088 (1982).
17. Couzin, I. D., Krause, J., James, R., Ruxton, G. D. & Franks, N. R. Collective memory and spacial sorting in animal groups. *Journal of Theoretical Biology* **218**, 1–11 (2002).

18. Inada, Y. & Kawachi, K. Order and Flexibility in the Motion of Fish Schools. *Journal of Theoretical Biology* **214**, 371–387 (2002).
19. Zheng, M., Kashimori, Y., Hoshino, O., Fujita, K. & Kambara, T. Behavior pattern (innate action) of individuals in fish schools generating efficient collective evasion from predation. *Journal of Theoretical Biology* **235**, 153–167 (2005).
20. Hildenbrandt, H., Carere, C. & Hemelrijk, C. K. Self-organized aerial displays of thousands of starlings: A model. *Behavioral Ecology* **21**, 1349–1359 (2010).
21. Papadopoulou, M., Hildenbrandt, H., Sankey, D. W. E., Portugal, S. J. & Hemelrijk, C. K. Self-organization of collective escape in pigeon flocks. *PLOS Computational Biology* **18**, e1009772 (2022).
22. Reynolds, C. W. Flocks, herds and schools: A distributed behavioral model. *ACM SIGGRAPH Computer Graphics* **21**, 25–34 (1987).
23. Hemelrijk, C. K. & Hildenbrandt, H. Diffusion and topological neighbours in flocks of starlings: Relating a model to empirical data. *PLoS ONE* **10**, 1–12 (2015).
24. Papadopoulou, M., Hildenbrandt, H. & Hemelrijk, C. K. Diffusion during collective turns in bird flocks under predation. *Frontiers in Ecology and Evolution* **11**, (2023).
25. Costanzo, A. & Hemelrijk, C. K. Spontaneous emergence of milling (vortex state) in a Vicsek-like model. *Journal of Physics D: Applied Physics* **51**, (2018).
26. Hemelrijk, C. K. & Hildenbrandt, H. Some causes of the variable shape of flocks of birds. *PLoS ONE* **6**, (2011).
27. Hemelrijk, C. K. & Hildenbrandt, H. Schools of fish and flocks of birds: their shape and internal structure by self-organization. *Interface Focus* **2**, 726–737 (2012).
28. Hemelrijk, C. K., Costanzo, A., Hildenbrandt, H. & Carere, C. Damping of waves of agitation in starling flocks. *Behavioral Ecology and Sociobiology* **73**, (2019).
29. Couzin, I. D. & Krause, J. Self-Organization and Collective Behavior in Vertebrates. *Advances in the Study of Behavior* **32**, 1–75 (2003).
30. Romano, D., Donati, E., Benelli, G. & Stefanini, C. A review on animal–robot interaction: from bio-hybrid organisms to mixed societies. *Biol Cybern* **113**, 201–225 (2019).
31. Storms, R. F. *et al.* Deterrence of birds with an artificial predator, the RobotFalcon. *Journal of The Royal Society Interface* **19**, 20220497 (2022).
32. Grimm, V. *et al.* Pattern-oriented modeling of agent-based complex systems: Lessons from ecology. *Science* **310**, 987–991 (2005).
33. McCreery, H. F., Gemayel, G., Pais, A. I., Garnier, S. & Nagpal, R. Hysteresis stabilizes dynamic control of self-assembled army ant constructions. *Nat Commun* **13**, 2 (2022).

34. Davis, J. M. The coordinated aerobatics of dunlin flocks. *Animal Behaviour* **28**, 668–673 (1980).
35. Buchanan, J. B., Schick, C. T., Brennan, L. A. & Herman, S. G. Merlin Predation on Wintering Dunlins: Hunting Success and Dunlin Escape Tactics. *The Wilson Bulletin* **100**, 108–118 (1988).
36. Ballerini, M. *et al.* Interaction ruling animal collective behavior depends on topological rather than metric distance: Evidence from a field study. *Proceedings of the National Academy of Sciences* **105**, 1232–1237 (2008).
37. Herbert-Read, J. E. *et al.* How predation shapes the social interaction rules of shoaling fish. *Proceedings of the Royal Society B: Biological Sciences* **284**, (2017).
38. Delm, M. M. Vigilance for predators: detection and dilution effects. *Behavioral Ecology and Sociobiology* **26**, 337–342 (1990).
39. Zoratto, F. *et al.* Behavioural response of European starlings exposed to video playback of conspecific flocks: Effect of social context and predator threat. *Behavioural Processes* **103**, 269–277 (2014).
40. Sridhar, V. H. *et al.* The geometry of decision-making in individuals and collectives. *Proceedings of the National Academy of Sciences* **118**, e2102157118 (2021).
41. Sarfati, R., Hayes, J. C. & Peleg, O. Self-organization in natural swarms of Photinus carolinus synchronous fireflies. *Science Advances* **7**, eabg9259 (2021).
42. Duffield, C. & Ioannou, C. C. Marginal predation: Do encounter or confusion effects explain the targeting of prey group edges? *Behavioral Ecology* **28**, 1283–1292 (2017).
43. Olson, R. S., Hintze, A., Dyer, F. C., Knoester, D. B. & Adami, C. Predator confusion is sufficient to evolve swarming behaviour. *Journal of the Royal Society, Interface* **10**, 20130305 (2013).
44. Zoratto, F., Carere, C., Chiarotti, F., Santucci, D. & Alleva, E. Aerial hunting behaviour and predation success by peregrine falcons Falco peregrinus on starling flocks Sturnus vulgaris. *Journal of Avian Biology* **41**, 427–433 (2010).
45. Gerlotto, F., Bertrand, S., Bez, N. & Gutierrez, M. Waves of agitation inside anchovy schools observed with multibeam sonar: a way to transmit information in response to predation. *ICES Journal of Marine Science* **63**, 1405–1417 (2006).
46. Doran, C. *et al.* Fish waves as emergent collective antipredator behavior. *Current Biology* **32**, 708-714.e4 (2022).
47. Lukas, J. *et al.* Multispecies collective waving behaviour in fish. *Philosophical Transactions of the Royal Society B: Biological Sciences* **378**, 20220069 (2023).
48. Romey, W. L. & Lamb, A. R. Flash Expansion Threshold in Whirligig Swarms. *PLOS ONE* **10**, e0136467 (2015).
49. King, A. J. *et al.* Selfish-herd behaviour of sheep under threat. *Current Biology* **22**, R561–R562 (2012).
50. Herbert-Read, J. E., Ward, A. J. W., Sumpter, D. J. T. & Mann, R. P. Escape path complexity and its context dependency in Pacific blue-eyes (Pseudomugil signifer). *The Journal of Experimental Biology* **220**, 2076–2081 (2017).

51. Cresswell, W. Escape responses by redshanks, Tringa totanus, on attack by avian predators. *Animal Behaviour* vol. 46 609–611 (1993).
52. Domenici, P. Context-dependent variability in the components of fish escape response: Integrating locomotor performance and behavior. *Journal of Experimental Zoology Part A: Ecological Genetics and Physiology* **313 A**, 59–79 (2010).
53. Marras, S., Killen, S. S., Claireaux, G., Domenici, P. & McKenzie, D. J. Behavioural and kinematic components of the fast-start escape response in fish: Individual variation and temporal repeatability. *Journal of Experimental Biology* **214**, 3102–3110 (2011).
54. Mills, R., Hildenbrandt, H., Taylor, G. K. & Hemelrijk, C. K. Physics-based simulations of aerial attacks by peregrine falcons reveal that stooping at high speed maximizes catch success against agile prey. *PLoS Computational Biology* **14**, 1–38 (2018).
55. Lima, S. L. & Dill, L. M. Behavioral decisions made under the risk of predation: a review and prospectus. *Canadian Journal of Zoology* **68**, 619–640 (1990).
56. Janosik, S. M. Towards an integrated view of escape decisions in birds under variable levels of predation risk. *University of Tartu Press* vol. 42 (2005).
57. Bode, N. W. F., Faria, J. J., Franks, D. W., Krause, J. & Wood, A. J. How perceived threat increases synchronization in collectively moving animal groups. *Proceedings of the Royal Society B: Biological Sciences* **277**, 3065–3070 (2010).
58. Papadopoulou, M. *et al.* Dynamics of collective motion across time and species. *Philosophical Transactions of the Royal Society B: Biological Sciences* **378**, 20220068 (2023).
59. Grimm, V. *et al.* The ODD protocol for describing agent-based and other simulation models: A second update to improve clarity, replication, and structural realism. *Jasss* **23**, (2020).
60. Tump, A. N., Wolf, M., Romanczuk, P. & Kurvers, R. H. J. M. Avoiding costly mistakes in groups: The evolution of error management in collective decision making. *PLOS Computational Biology* **18**, e1010442 (2022).
61. Ebert, D. S., Musgrave, F. K., Peachey, D., Perlin, K. & Worley, S. *Texturing & Modeling: A Procedural Approach*. (Morgan Kaufmann, 2003).

Acknowledgements

The authors would like to thank the group of self-organization of social systems at the University of Groningen for their support and comments at various stages of this project. This work has been financed by the Netherlands Organisation for Scientific Research (NWO - https://www.nwo.nl), the Open Technology Program (OTP) "Preventing bird strikes: Developing RoboFalcons to deter bird flocks" (project number 14723) awarded to C.K.H.

Author contributions

MP, HH, and CKH conceptualized the study. RS collected the empirical data. MP and RS analyzed the empirical data. MP and HH developed the computational model. MP designed the computational experiments, ran the simulations, analyzed the simulated data, created all visualizations, and wrote the original manuscript. All authors provided feedback and revised the manuscript.

Competing interest statement

The authors declare no competing interests.

Data and code availability

The StarEscape model will be available on a GitHub repository and the version used to reproduce the data presented here will be archived on a Zenodo repository. All simulated data and further code to analyze the data exported by the model as used here will also be available online upon publication.